Self-Assembling Platonic and Archimedean Solids: Innovations and Advancements

Donald J. Plante[1] and John R. Jungck[2]

[1]University of New Hampshire at Manchester, Manchester, NH, USA; donald.plante@unh.edu
[2]University of Delaware, Newark, DE, USA; jungck@edel.edu

Abstract

Previous studies have employed 3D-printed spherical models inspired by the geometry of the dodecahedron to demonstrate the mechanism of self-assembly of viral capsids from free-floating capsomeres. This research builds on these studies by constructing a complete set of 3D-printed self-assembling Platonic solids. These objects not only serve a functional purpose but are also aesthetically pleasing as they showcase the duals of each solid. Additionally, we expand upon the complexity of previous methods by creating three self-assembling Archimedean solids; the truncated tetrahedron, truncated octahedron, and truncated icosahedron.

Introduction

Self-assembly, the spontaneous organization of individual components into ordered structures, is a rapidly advancing field of study with applications in many areas from engineering and biology to mathematics. Self-assembly was demonstrated in the context of viral capsids by Olson et al. [4] who utilized 3D-printed components in combination with magnets to create models that self-assemble when placed into a container and shaken. Their model was based on the geometry of the dodecahedron with 12 individual components representing the capsomeres of a virus. This work provided valuable insights into the mechanism of self-assembly of spherical viral capsids [3].

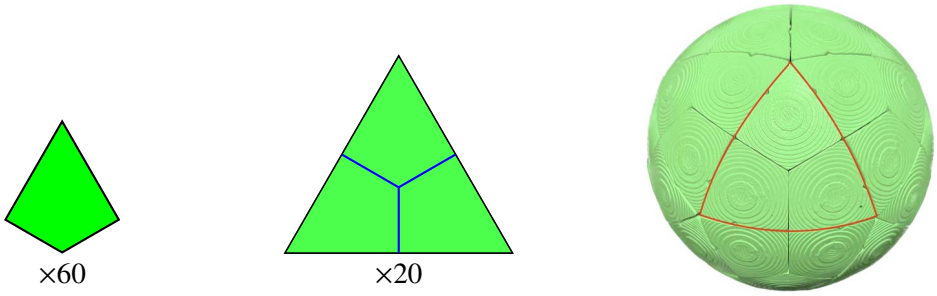

Figure 1: *(a) T=1 icosahedral asymmetric quadrilateral unit, (b) triangular face composed of 3 quadrilateral units, and (c) T=1 viral capsid model composed of 60 quadrilateral units. The red outline highlights one of the original triangular faces of the spherical icosahedron.*

In this article, we describe recent progress in our research on self-assembling spherical models, building on the method first demonstrated by Olson et al [4]. Recently, we have successfully created self-assembling models based on spherical versions of the five Platonic solids. In our previous work [3], we designed and fabricated a 3D-printed self-assembling structure using the principles of Caspar-Klug theory [1]. The

structure was modeled after a viral capsid and had a triangulation number of $T = 1$, as depicted in Figure 1. This model is the foundational case for the classification and enumeration of other icosahedral structures. It consists of 60 identical quadrilateral subunits and represents the simplest possible icosahedral triangulation number.

Self-Assembling Platonic Polyhedra

One way in which the $T = 1$ model can be understood, is as the union of the vertices and edges from a spherical icosahedron with its dual polyhedron, the spherical dodecahedron. Thinking about the $T = 1$ model in this way led us to explore how we could artistically represent the concept of dual polyhedra in each of the self-assembling spherical Platonic solids. In Figure 2 below, each of the Platonic solids has been 3D-printed in two distinct colors using PLA filament on an Ultimaker 3 3D-printer. The first color of each model depicts the solid itself, while the second color is used to visually represent its dual by forming arcs on the spherical surface that start at the center of each face and connect to the middle of each edge. This approach provides a clear visual representation of the dual of each solid once it has been assembled. Since the dual of the icosahedron is the dodecahedron and vice versa, they are colored in the same two colors, with opposite colors indicating which one shows the dual. This is also true for the cube and octahedron. As the tetrahedron is self-dual, only one model is required, featuring its chosen two complementary colors. By examining the edges of each component as well as the colored dual lines, the geometry of the $T = 1$ model can be observed in both the dodecahedron and the icosahedron models. This is most easily seen in the icosahedron model on the far right of Figure 2, where each component triangle has dual lines in the same location as the red lines in Figure 1(b).

Figure 2: *The five self-assembling spherical Platonic solids are 3D-printed to visually represent their duals, with an individual component displayed in front. Left to right: The Tetrahedron, Cube, Octahedron, Dodecahedron, and Icosahedron*

Self-Assembling Archimedean Polyhedra

An additional goal of this paper is to showcase how we've expanded the capabilities of 3D-printed self-assembling models by creating models with multiple face types. We present here for the first time, three additional 3D-printed self-assembling models from the collection of spherical Archimedean solids as shown in Figure 3: the truncated tetrahedron, truncated octahedron, and truncated icosahedron, also known colloquially as the soccer ball. Using these models we illustrate the methods used to create self-assembling spherical models with multiple face types and further demonstrate the potential of self-assembly using 3D-printing

technology. By extending our research into more complex geometries, we aim to gain new insights into the processes that guide self-assembling structures. You can observe the self-assembly process of selected models discussed in this paper by visiting the following link: https://qubeshub.org/publications/4262/1[5].

(a) (b) (c)

Figure 3: *3D-printed self-assembling spherical Archimedean solids. (a) The truncated tetrahedron, (b) Truncated octahedron, and (c) Truncated icosahedron*

General Design Process

Each of our self-assembling solids are created following a multistep process. This involves using CAD software such as Fusion 360 to complete the following steps:

1. A solid is radially projected onto the surface of a sphere.
2. The projected faces are thickened to create an individual component.
3. Holes are made on the side of the edges of each component to accommodate 3mm cylindrical magnets.
4. A magnet map is created that allows only correct connections to form during the assembly process.
5. 3 mm diameter neodymium magnets are glued into place following the magnet map.
6. The collection of subunits are shaken in a spherical container to self-assemble the final polyhedron.

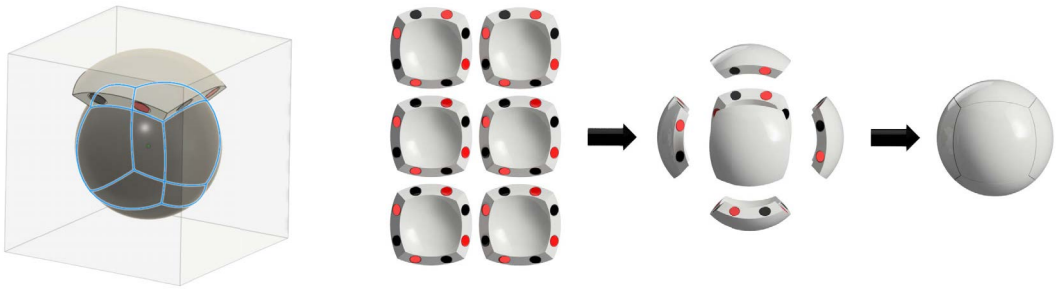

(a) (b)

Figure 4: *Creation of a self-assembling spherical cube: (a) The cube is radially projected onto a sphere, the faces are thickened in a radial direction, and (b) a magnet map shows the assembly process.*

In Figure 4 we see the creation of the spherical cube using the steps outlined above. Our easiest way to create a magnet map for each of the Platonic solids that causes them to self-assemble is an alternating polarity pattern

around the edges of the components, as shown in Figure 4(c). However, when creating a self-assembling model with two or more face types, a more complex magnet map is required.

Self-Assembling Truncated Icosahedron

Truncating any of the Platonic solids results in a new geometric solid with two distinct face types. To illustrate the creation of our truncated models we focus on the design of the spherical truncated icosahedron. This solid has 12 identical pentagonal faces and 20 identical hexagonal faces. The addition of a second face type to our previously developed models necessitates a more complicated magnet map than that used for the Platonic solids. Furthermore, it also requires that we slightly change the physical shape of each component to avoid certain interactions.

To design a working magnet map we consider the rotational icosahedral group [2], denoted by I, to help us understand the symmetries of the truncated icosahedron and its faces. This group can be used to describe the rotational symmetries of the icosahedron as well as the truncated icosahedron. It is a discrete group, of order $|I| = 60$. The rotational icosahedral group I is generated by a set of rotations, that preserve the geometry of the icosahedron.

For the construction of a working magnet map, we use the subgroups of I that preserve the hexagonal and pentagonal faces of a truncated icosahedron. The subgroup of I that preserves the hexagonal faces is isomorphic to the cyclic group of order 3, denoted as C_3. Similarly, the subgroup of I that preserves the pentagonal faces is isomorphic to the cyclic group of order 5, denoted as C_5.

To better understand these subgroups in the context of the truncated icosahedron, it is worth noting that during the truncation process, the hexagonal faces of the truncated icosahedron inherit a 3-fold symmetry from the faces of the original icosahedron. Specifically, each hexagonal face of the truncated icosahedron is centered at the same location as a former triangular face of the icosahedron, which had a 3-fold symmetry around its center. Similarly, the pentagonal faces of the truncated icosahedron inherit a 5-fold rotational symmetry around each face center. This is because they are formed by truncating the vertices of an icosahedron, which have a 5-fold symmetry centered about them.

Using this information, we design our components and magnet maps to have a 3-fold rotational symmetry about the center of each hexagonal face and a 5-fold rotational symmetry about the center of each pentagonal face. This approach enhances the probability that the resulting components will assemble correctly into a spherical truncated icosahedron.

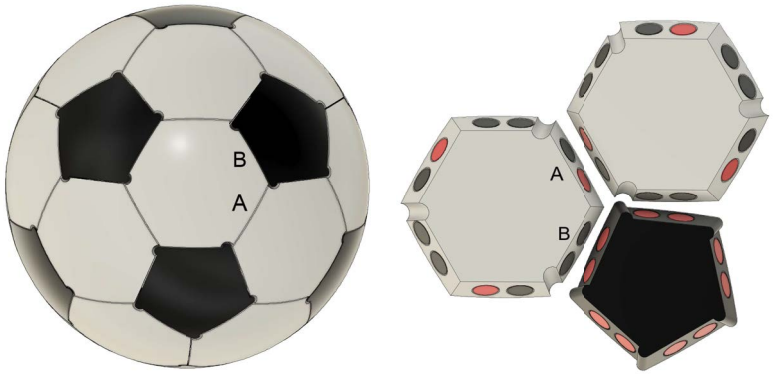

(a) (b)

Figure 5: *(a) Self-assembling truncated icosahedron with two edge types, A and B (b) Hexagonal and pentagonal components viewed from the bottom with magnet map for edge types A and B.*

To create a useable magnet map it is also important to consider how these symmetries contribute to the edge interactions between the pentagonal and hexagonal faces. As shown in Figure 5, there are two distinct edge types in a truncated icosahedron. Edge A is shared by two adjacent hexagons, while edge B is shared between a hexagon and an adjacent pentagon. Edge A can be thought of as a shortened version of the original edges in the icosahedron model, and thus an alternating north (red) pole, south (black) pole arrangement on these edges still ensures proper component connections. For edge B, which is created in the process of truncating the original icosahedron, three additional considerations must be taken into account. Reversing the pattern of alternating magnets we used on edge A would not work, as edge B would be attracted to edge A in an upside-down orientation.

In addition, the magnet map must ensure that all pentagons repel each other, as none are connected in the final model. To achieve this, we have oriented all magnets on the sides of the pentagonal pieces such that their north pole (red) is facing outward. This leaves the corresponding edge B on the hexagonal pieces with their south pole (black) facing outward. One potential issue with this arrangement is that the hexagonal and pentagonal components are attracted to each other in an upside-down orientation. To prevent this incorrect attachment, we have added a knob and notch to the side of edge B that only allows the two piece types to connect in the proper orientation.

Design Considerations for 3D-Printing

During the construction process of these models, we've discovered that partially assembled portions of smaller models exhibit greater stability, resulting in a higher likelihood of achieving full assembly in comparison to larger versions of the same model. Smaller pieces are less likely to be shaken loose during the assembly process, as they have less leverage to break loose when they collide with the sides of the container that they are being shaken in. Additionally, with smaller pieces, the size of the magnets in relation to the components is greater, resulting in a stronger hold. These advantages for smaller components results in a final design that is less likely to break apart during the assembly process. In particular, when attempting to make self-assembling models greater than about 60 mm in diameter the model would continually break apart before full assembly was complete. This limit on the diameter of the final model determines the maximum number of components that can be used to create a self-assembling sphere. In general, as the number of component pieces increases so does the corresponding diameter of the final object. This puts an upper limit on this method if one is to use magnets of the size we have chosen. Although it is possible to use smaller magnets that would fit into corresponding smaller components we are limited in size by the dimensions of cheaply available magnets. In addition, we have found that if the component pieces are too small, they tend to clump together as a single mass.

An additional consideration when designing these models is the amount of work that is required to construct them after they are 3D-printed. To help with the post processing of the models, we have designed each component piece to have a flat bottom, as seen in Figure 6(a), so that they are able to be printed without the need for support material or additional adhesion such as a brim or raft. This has the unintended but mathematically interesting consequence that while the outside of the model is a sphere, its interior is the original polyhedron with flat faces.

In addition, gluing many small magnets into each component is challenging. The truncated icosahedron model contains 90 edges, each of which require 4 magnets, for a total of 360. The magnets used were 3mm in diameter and 2mm in height making them extremely tedious to assemble by hand. To overcome these issues and account for our 3D-printer's tolerance, we designed the diameter of each magnet hole to be 0.3 mm larger than the diameter of the magnets. This allows the magnets to be pressed into place so that it is not necessary to hold them while the super glue dries. We also designed color coded tools, shown in Figure 6(b), to quickly orient the magnets for north and south polarity and insert them into the 3D-printed components.

(a) (b)

Figure 6: *(a) Hexagonal component with a flat interior face, shown in a side view, designed for ease of 3D-printing, (b) North- and south-oriented magnet tools*

Summary and Conclusions

In conclusion, we have shown a method for creating both self-assembling spherical Platonic solids with a single face type as well as self-assembling spherical Archimedean solids with two face types. Although we have focused on the spherical truncated icosahedron throughout, these same principles were used in the design and assembly of the truncated tetrahedron and truncated octahedron shown in Figure 3. We would like to complete this set of the truncated Platonic solids by creating models based on the truncated cube, and truncated dodecahedron. In addition, we hope to continue pushing the bounds of this research by constructing a self-assembling model that has three distinct face types. Currently, we have had partial success with a self-assembling spherical model of the truncated cuboctahedron. The truncated cuboctahedron is an Archimedean solid consisting of 12 square faces, 8 hexagonal faces, and 6 octagonal faces. We anticipate that incorporating a third face type into the design will require us to use a more complex magnet mapping strategy in order to successfully achieve self-assembly of the model.

Not only is this research important for its practical applications and understanding of fields such as virology, biomimetic drug delivery, and engineering, but it also presents a fun and artistic mathematical challenge. We believe pushing this research in new ways will lead to even more exciting and dynamic self-assembling designs. We look forward to continuing to explore and develop this method in the future.

References

[1] D. L. D. Caspar, and A. Klug. “Physical principles in the construction of regular viruses.” *Cold Spring Harb Symp Quant Biol.*, vol. 27, 1962, pp. 1-24. https://pubmed.ncbi.nlm.nih.gov/14019094/

[2] N. W. Johnson. *Geometries and Transformations*, “Chapter 11: Finite symmetry groups.” Cambridge University Press, 2018.

[3] J. R. Jungck, S. Brittain, D. Plante, and J. Flynn. “Self-Assembly, Self-Folding, and Origami: Comparative Design Principles.” *Biomimetics*, vol. 8, no. 1, 2022. https://www.mdpi.com/2313-7673/8/1/12

[4] A. J. Olson, Y. H. E. Hu, and E. Keinan. “Chemical mimicry of viral capsid self-assembly.” *Proceedings of the National Academy of Sciences*, vol. 104, no. 52, 2007, pp. 20731-20736. https://www.pnas.org/doi/abs/10.1073/pnas.0709489104

[5] D. Plante, and J. R. Jungck. *Self-Assembling Geometric Solids Videos*. QUBES Educational Resources. 2023. http://dx.doi.org/10.25334/40S6-ZY53